JOURNAL OF MATERIALS SCIENCE 21 (1986) 1990–1996

The metallography of a cobalt-based implant alloy after solution treatment and ageing

R. N. J. TAYLOR*, R. B. WATERHOUSE
Department of Metallurgy and Materials Science, The University of Nottingham, Nottingham NG7 2RD, UK

The ageing characteristics of a commercial Co–Cr–Mo–C alloy after solution treatment were investigated using optical and electron microscopy. An $M_{23}C_6$-type carbide was identified by X-ray and electron diffraction after ageing treatments between 650 and 1150° C. Nucleation and growth of this carbide took place on intrinsic stacking faults by Suzuki segregation in the cobalt matrix. High stacking-fault densities gave rise to intragranular striations which were visible after etching once precipitation had occurred. Ageing temperatures of 925° C and above increased the stability of the f c c cobalt matrix and led to precipitation on undissociated dislocations. Grain-boundary carbides were evident at all ageing temperatures.

1. Introduction

The precipitation mechanisms of an $M_{23}C_6$-type carbide (where M = Co, Cr, Mo) have been discussed during the ageing of a Co–Cr–Mo–C implant alloy in the production solution-treated condition [1]. An extra solution treatment at 1250° C for 2 h followed by a water quench not only reduced the amount of residual carbide from the investment casting operation, but also altered the ageing response of the alloy.

Three types of precipitation reaction were seen on ageing the production solution-treated alloy [1]. At low (925° C) temperatures, fine carbides grew in interdendritic positions within the grains as a result of residual coreing from the casting operation. Transmission electron microscopy (TEM) showed the $M_{23}C_6$ to have nucleated upon intrinsic stacking faults which became abundant due to the metastability of the f c c cobalt matrix. Extensive carbide growth was limited by the diffusion of chromium and molybdenum, but was assisted by a discontinuous reaction which occurred at some grain boundaries. The boundaries acted as sinks for solute atoms with increased diffusion rates and gave rise to a lamellar morphology. Electron diffraction across the lamellae showed $M_{23}C_6$ in f c c α-cobalt, thereby dispelling the possibility of a eutectoid reaction.

Ageing temperatures of 925° C and above changed the precipitation mechanism from stacking-fault nucleated to dislocation nucleated, due to the increased thermodynamic stability of the f c c allotrope. At all temperatures a cube/cube relationship was found to exist between the carbide and the matrix so that

$$\{1\,1\,1\}_{\text{fcc Co}} \| \{1\,1\,1\}_{M_{23}C_6}$$

and

$$\langle 1\,1\,0\rangle_{\text{fcc Co}} \| \langle 1\,1\,0\rangle_{M_{23}C_6}$$

Growth took place predominantly on the $\{1\,1\,1\}$ planes since these showed the least mismatch over the $\{1\,1\,0\}$ and $\{1\,0\,0\}$ planes.

The majority of previous work had been performed by The National Advisory Comittee for Aeronatics (NACA) on the ageing of wrought HS21 which had been solution treated at 1230° C and above [2–6]. Intragranular striations were reported in these experiments and were attributed to slip lines which had formed from the thermal stresses set up by the water quench of the solution treatment. TEM performed by Vande Sande *et al.* (7) showed martensitic bands of h c p Co (ε) phase in both wrought and cast solution-treated HS21. The transformation markings were clearly visible in the former under optical microscopy but apparently not in the cast alloy. Precipitation of $M_{23}C_6$, which occurred on ageing at 650 and 750° C in these samples, tended to be associated with the martensitic bands. The basal $\{0\,0\,1\}$ planes were aligned with the $\{1\,1\,1\}$ planes of both the $M_{23}C_6$ and the α-cobalt.

Therefore the intragranular striations observed in this class of treatment have had two mechanisms proposed for their formation [6, 7]. The cobalt matrix would have contained more chromium and molybdenum after the extra solution treatment, and these elements promote the ε form on the evidence of the binary equilibrium diagram [8]. This would endorse the mechanism involving the allotropic transformation, although the increased carbon content would have the reverse effect. The purpose of this study was therefore not only to complement the work performed on the production solution-treated material, but also to classify the nature of the intragranular striations. In addition it was hoped that the increased homogeneity of the solute atom distribution might lead to more advantageous mechanical properties after ageing.

*Present address: AWRE, Aldermaston, Reading, UK.

0022–2461/86 $03.00 + .12

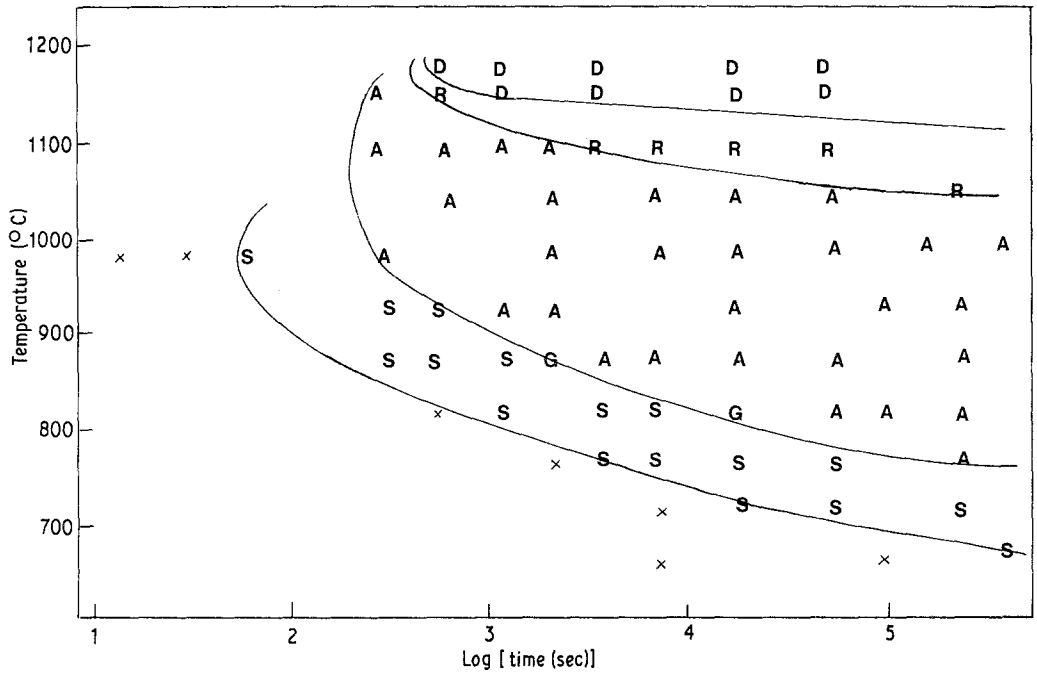

Figure 1 Time–temperature–precipitation (TTP) diagram on ageing the solution heat-treated material. (x) Grain boundaries only, (S) intragranular striations, (G) grain-boundary carbides present, (A) change to a blocky morphology, (R) spheroidization of the precipitates, (D) dissolution.

2. Experimental procedure

The heat treatments were carried out in a tube furnace supplied with a purified, dried argon atmosphere. A Pt/Pt 13% Rh thermocouple controlled the temperature in the hot zone to $\pm 3°$ C. The solution treatment consisted of a 2 h soak at 1250° C followed by water quenching. After ageing all specimens were rapidly quenched in water.

Metallographic examination was carried out optically and under scanning electron microscopy (SEM) after removing $\simeq 1$ mm of the surface and polishing down to 1 μm diamond and electrolytically etching in 5% HNO_3 in ethanol. Electrolytic extraction of the carbides was carried out in this solution [1].

The preparation of thin foils for TEM demanded great care due to the rapid work-hardening characteristics of the alloy. 3 mm diameter discs were trepanned out by a spark erosion technique. Only a limited amount of grinding was possible, and final thinning was performed in a jet electropolisher using an electrolyte recommended by Yukawa *et al.* ([9], their Table II) with a current density of 2 to 2.5 $\times$ 10^{-7} A m^{-2} (30 to 35 mA). Any perforated foils which were unsatisfactory were further thinned using ion-beam bombardment. This was extremely slow and could only be used on foils which had previously been electropolished.

The age-hardening response was determined using a Vickers pyramidal diamond tester with a 20 kg load.

3. Results and discussion

3.1. Precipitate analysis

X-ray diffraction patterns of electrolytically extracted particles taken from a number of heat treatments showed only the $M_{23}C_6$ type carbide ($a = 1.065$ nm). This was supported by numerous electron diffraction patterns, which also indicated that a cube/cube relationship existed between the carbide and the fcc cobalt matrix so that

$$\{1\,1\,1\}_{\text{fcc Co}} \| \{1\,1\,1\}_{M_{23}C_6}$$

$$\langle 1\,1\,0\rangle_{\text{fcc Co}} \| \langle 1\,0\,0\rangle_{M_{23}C_6}$$

and

$$\{1\,0\,0\}_{\text{fcc Co}} \| \{1\,0\,0\}_{M_{23}C_6}$$

Compositional shifts in the chromium, molybdenum and cobalt content of the carbide were revealed by EDXA. The growing carbide exhibited higher concentrations of the solute atoms (chromium and molybdenum) which increased with ageing time and temperature. The grain-boundary carbides usually contained more molybdenum than those situated elsewhere in the microstructure.

3.2. Metallography

In addition to a reduction in the size and number of residual interdendritic carbides, the grain size was also

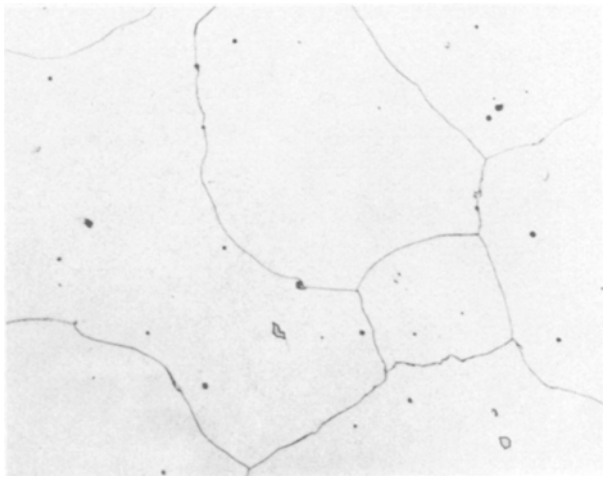

Figure 2 Aged at 815° C for 5 min (× 160). Recrystallized grains evident.

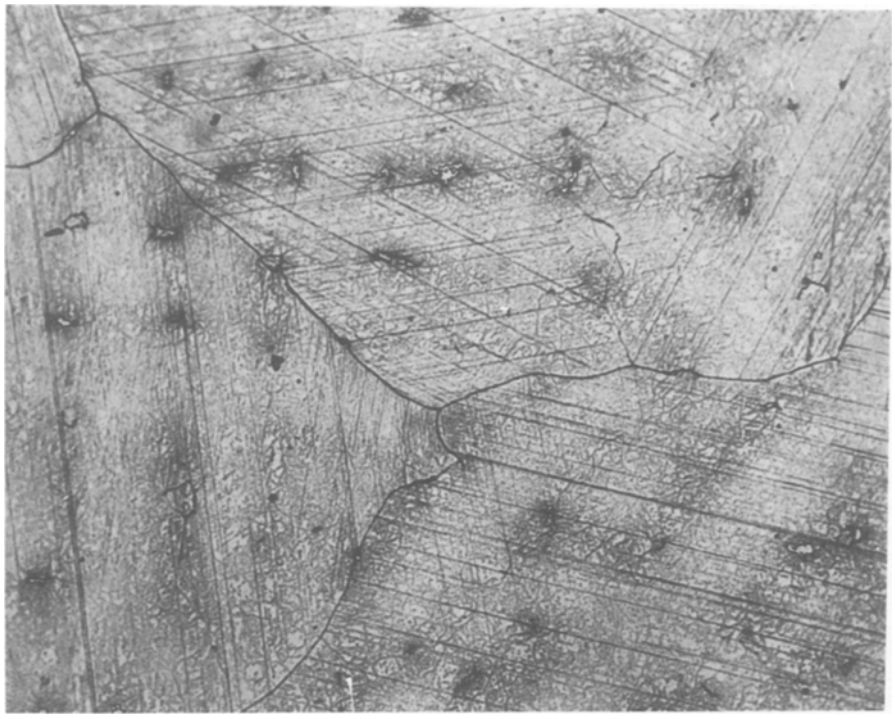

Figure 3 Aged at 760° C for 5 h (× 200). Intergranular striations and dense, relatively homogeneous precipitate. Some residual blocky carbides present.

considerably increased by the extra solution treatment.

It was found that similar ageing times and temperatures were required for precipitation as the production solution-treated alloy [1]. A time–temperature–precipitation (TTP) diagram is shown in Fig. 1, and indicates the various changes in morphology of the $M_{23}C_6$ carbide on ageing. Examination of specimens outside the boundary representing the onset of precipitation in Fig. 1 showed that recrystallization had taken place (Fig. 2). Where precipitation had occurred three factors were significant.

Firstly, intragranular striations appeared which became thicker and more discontinous as ageing proceeded and the temperature increased (Figs 3 to 6). Secondly the precipitation in the grains was more homogeneous than in the aged production solution-treated specimens [1], although the characteristic dendritic pattern became evident after increased ageing time and temperature (Figs 5 and 6). A blocky carbide morphology also became apparent after extensive ageing, as shown in the TTP diagram. Finally, no precipitate was associated with the grain boundaries except in the form of blocky carbides at the higher ageing temperatures (Figs 5 to 7). Re-solution of the precipitate occurred at temperatures in excess of 1100° C (Fig. 7).

It was therefore apparent that differences had arisen

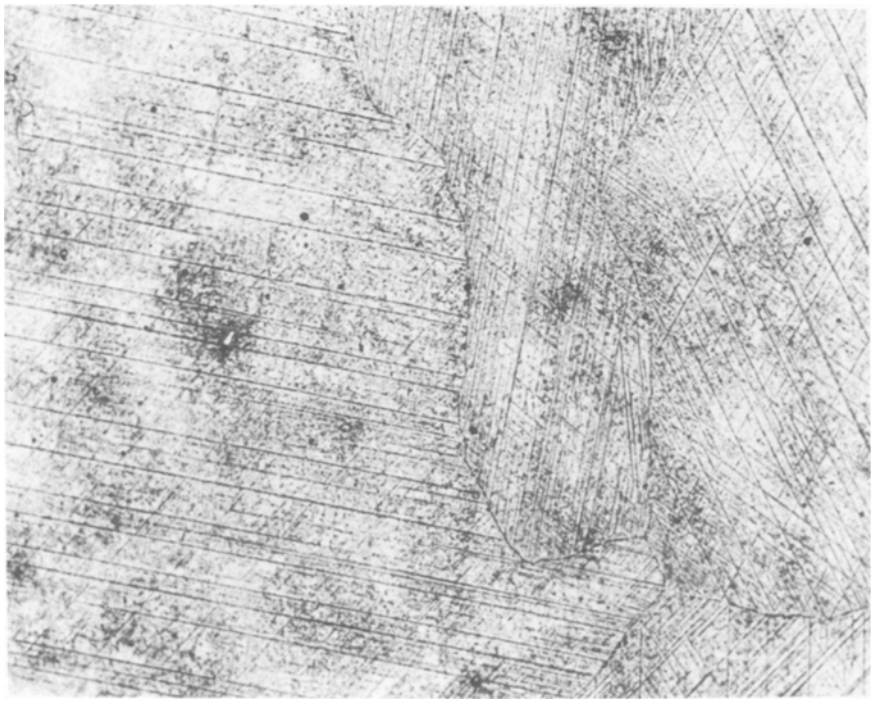

Figure 4 Aged at 870° C for 68 h (× 200). Less homogeneous distribution of precipitate.

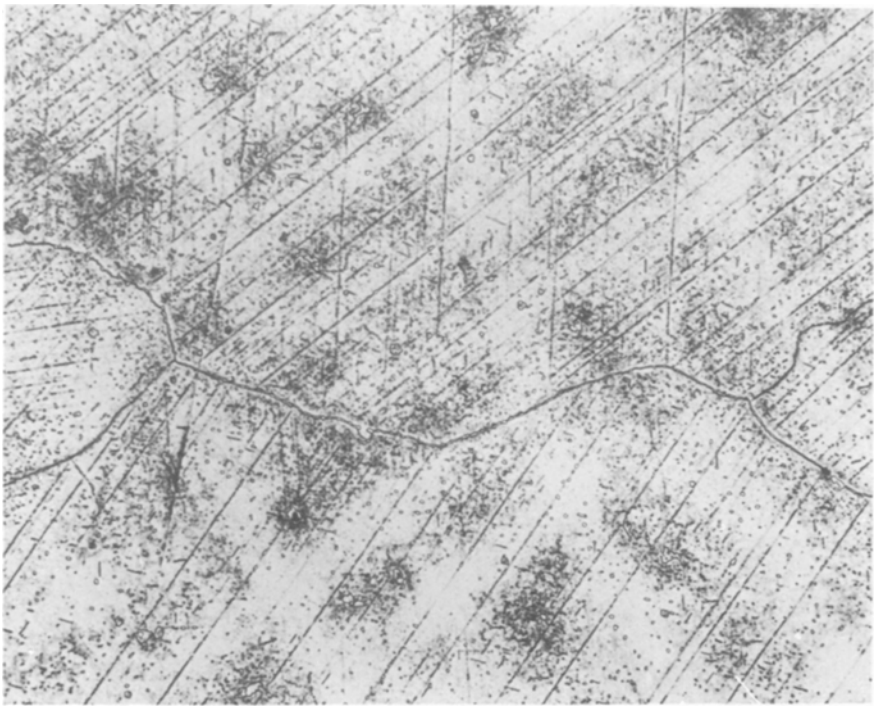

Figure 5 Aged at 980° C for 188 h (× 200). Coarse grain-boundary carbides, precipitation in interdendritic regions.

in the ageing response of the material after the extra solution treatment. These were clearly demonstrated by the presence of the intragranular striations and the absence of any lamellar morphology at the grain boundaries.

3.3. Transmission electron microscopy

The additional solution treatment gave rise to an increased density of intrinsic stacking fault, but no transformation from f c c to h c p cobalt was observed, apart from the presence of the stacking faults. In some areas their density was so great that h c p cobalt reflections appeared in the electron diffraction patterns. The intrinsic nature of the faults was determined by the method devised by Gevers, Art and Amelincx [10], although it was not possible to use this test where the fault density was high. However, to be in such concentrations the stacking fault must be intrinsic in nature, so that the driving force for the profuse dissociation was the allotropic transformation and the formation of h c p cobalt.

As ageing progressed, abundant precipitation became clearly visible in association with the stacking faults (Figs 8 and 9). It was evident that the intragranular striations observed under optical microscopy were composed of densely packed stacking faults and were only visible when carbide precipitation was associated with the faults. The random carbide distributions on the stacking faults, the uniform appearance of the bounding partial dislocations on the

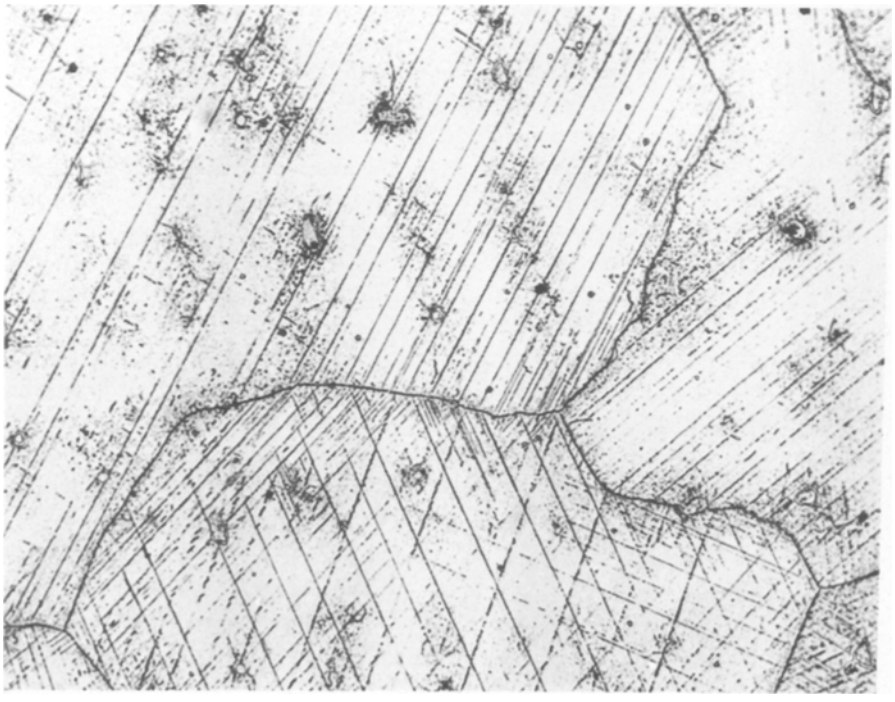

Figure 6 Aged at 1050° C for 5 h (× 200). Discontinuous striations of blocky carbide precipitate. Interdendritic pattern in the matrix.

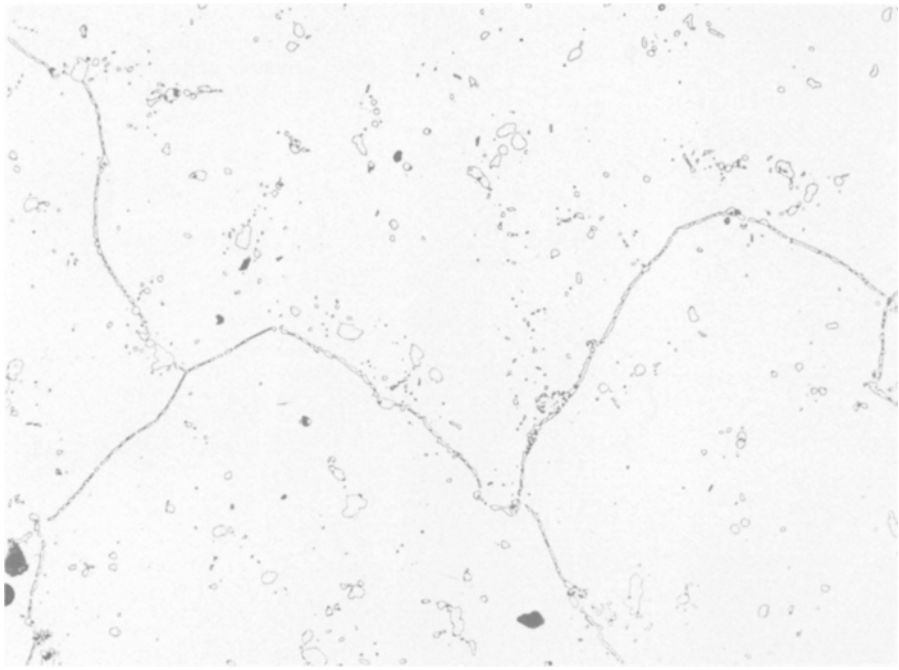

Figure 7 Aged at 1150° C for 16.5 h (× 200). Re-solution of precipitation.

stacking faults and the predominance of stacking-fault networks prior to precipitation suggested a mechanism of Suzuki segregation. The solute atoms diffuse to the stacking faults preferentially due to the difference in crystal structure. Calculations of the space packing and metal-atom volume of each allotropic form based on the crystallographic data available [11] indicated the hexagonal form to be marginally favourable for this preferential diffusion [12].

Various studies have observed the phenomenon of precipitation in association with stacking faults in alloys based on cobalt, nickel, aluminium and iron [13–18], although a variety of mechanisms was operating. Repeated nucleation of bounding Frank partial dislocations occurred in austenitic stainless steels [18] and Inconel 625 [15], whilst in some aluminium alloys hexagonal particles formed on intrinsic faults (after solute enrichment of the faults), thus reducing the interfacial energy associated with the precipitation [17]. However, in the system under study the carbide possessed a complex fcc structure [19], and in addition the fcc coballt {1 1 1} and hcp {0 0 0 1} were calculated to be identical in both atomic spacing and arrangement [12].

Ageing the alloy at temperatures in excess of 925° C showed a change in nucleation mechanism similar to that observed previously [1]. The stacking fault density decreased sharply, possibly due to an increase in the thermodynamic stability of the fcc allotrope, and as a result the $M_{23}C_6$ carbide nucleated on undissociated dislocations (Fig. 10). Growth took place on well-defined planes, predominantly the {1 1 1} planes, since these result in the least mismatch [12].

A change in nucleation mechanism from stacking faults to dislocations has been reported for the precipitation of NbC in some austenitic stainless steels [20–22]. The difference was attributed to the enhanced solute diffusion rates. This would have been a factor in the system under study, but, in addition, the reduced driving force for stacking-fault formation due to the increased stability of the fcc lattice must have had a significant effect.

3.4. Age-hardening response

The results of the hardness tests are shown in Fig. 11, plotted three-dimensionally by computer. Large increases were recorded after extensive ageing at 760 to 815° C. The high hardnesses were a result of the carbide dispersions on the stacking fault, and with the onset of dislocation-nucleated precipitation these increases diminished. This concurred with observations made on some austenitic stainless steels [23, 24].

4. Conclusions

The introduction of a further solution treatment on a production solution-treated Co–Cr–Mo–C investment-cast implant alloy altered the ageing response of the material. Nucleation and growth of $M_{23}C_6$-type carbides occurred in association with intrinsic stacking faults, as observed in the original alloy, but the increased homogeneity of the solute atoms precluded the necessity for any discontinuous reaction to occur at the grain boundaries. An increased stacking-fault density led to intergranular striations becoming apparent after precipitation had occurred on the stacking faults. At high (925° C) ageing temperatures the nucleation and growth mechanisms of the carbide were identical to those observed in the alloy without the additional solution treatment. Nucleation occurred on undissociated dislocations and growth took place on distinct crystallographic planes, of predominantly {1 1 1} type. A cube/cube relationship existed between the carbide and the fcc matrix at all temperatures between 650 and 1150° C. Maximum age-hardening occurred at 760 to 815° C.

Acknowledgements

The authors would like to express their gratitude to Howmedica Industries Inc. for the provision of the

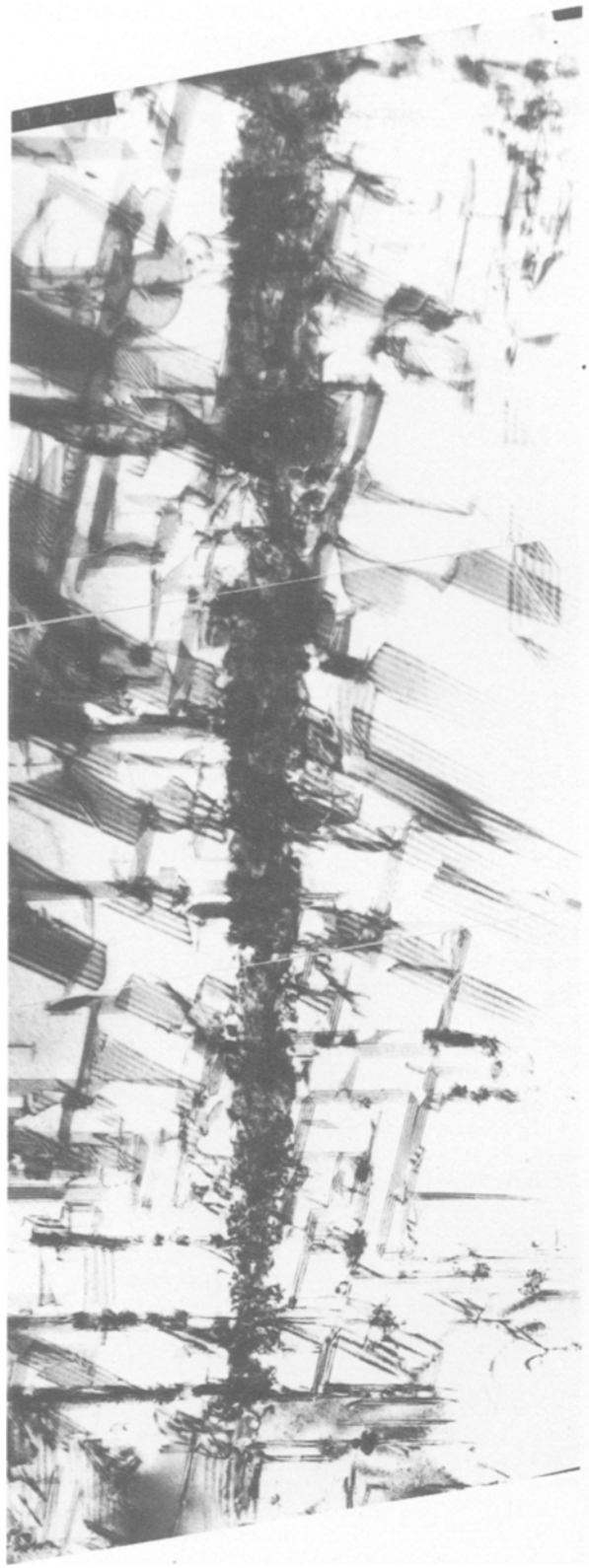

Figure 8 Aged at 815° C for 2 h (TEM × 43 000). Dense intrinsic stacking faults forming an intergranular striation.

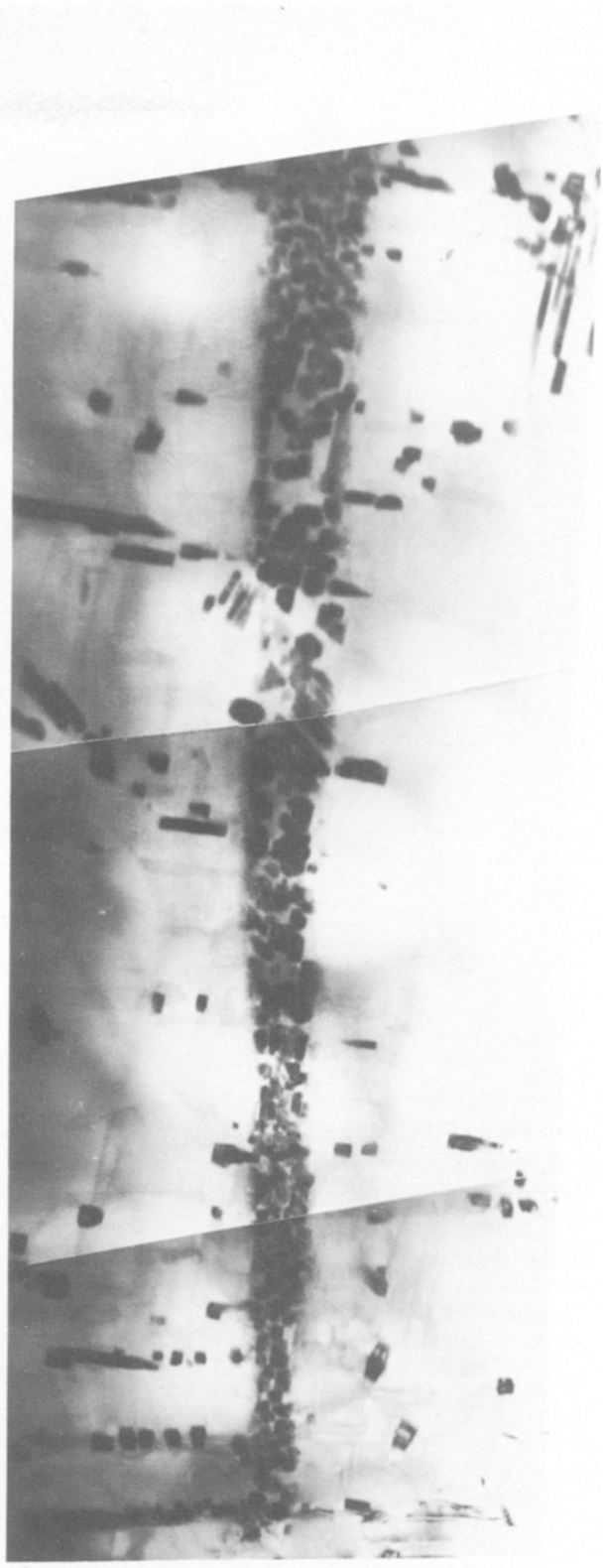

Figure 9 As Fig. 8, tilted to show carbide precipitation ($M_{23}C_6$-type) associated with the stacking fault. Note also the faceted features of the precipitate.

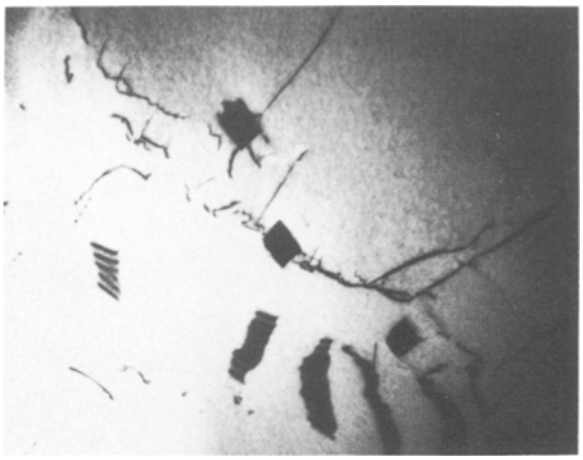

Figure 10 Aged at 980° C for 5 min (TEM × 30 600). Undissociated disclocations with carbide precipitates.

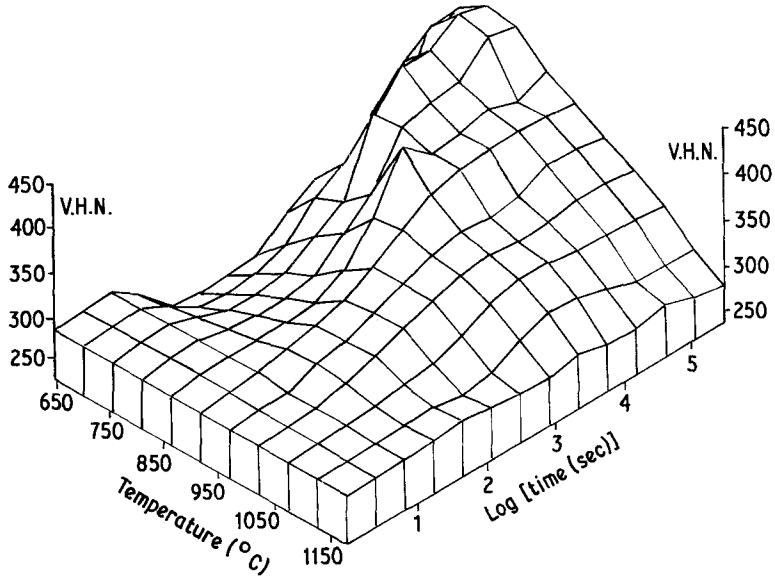

Figure 11 Hardness against ageing time and temperature.

material and the help and co-operation received. R. N. J. T. is also indebted to the Science and Engineering Research Council for the funding of this work.

References

1. R. N. J. TAYLOR and R. B. WATERHOUSE, *J. Mater. Sci.* **18** (1983) 3265.
2. F. J. CLAUSS and J. W. WEETON, NACA Technical Note 3107 (1954).
3. *Idem*, NACA Technical Note 3108 (1954).
4. J. W. WEETON and R. A. SIGNORELLI, NACA Technical Note 3109 (1954).
5. F. J. CLAUSS, F. B. GARRETT and J. W. WEETON, NACA Technical Note 3512 (1955).
6. J. W. WEETON and R. A. SIGNORELLI, *Trans. ASM*, **47** (1955) 815.
7. J. B. VANDE SANDE, J. R. COKE and J. WULFF, *Met. Trans.* **7A** (1976) 389.
8. A. GIAMEI, J. BURMA and E. J. FREISE, *Cobalt* **39** (1968) 88.
9. S. YUKAWA and K. SATO, *Trans. J. Inst. Metals* **9** (Suppl.) (1968) 680.
10. R. GEVERS, A. ART and S. AMELINCX, *Phys. Status Solidi* **3** (1963) 1563.
11. "The Cobalt Monograph", (Centre d'Information du Cobalt, Brussels, 1960) p. 76.
12. R. N. J. TAYLOR, PhD thesis, Nottingham University (1982).
13. P. A. BEAVEN, P. R. SWANN and D. R. F. WEST, *J. Mater. Sci.* **13** (1978) 691.
14. *Idem, ibid.* **14** (1979) 354.
15. B. E. JACOBSSEN, *Met. Trans.* **11A** (1980) 1167.
16. P. S. KOTVAL, *Trans. AIME* **242** (1968) 1651.
17. B. A. NOBLE and G. E. THOMPSON, *Met. Sci. J.* **8** (1972) 167.
18. J. M. SILCOCK and W. J. TUNSTALL, *Phil. Mag.* **10** (1964) 361.
19. H. J. GOLDSCHMIDT, *J. Iron Steel Inst.* **160** (4) (1948) 345.
20. J. S. T. VAN ASWEGAN, R. W. K. HONEYCOMBE and D. H. WARRINGTON, *Acta Metall.* **12** (1964) 1.
21. J. M. SILCOCK, *J. Iron Steel Inst.* **201** (1963) 409.
22. P. W. TEARE and N. T. WILLIAMS, *ibid.* **201** (1963) 125.
23. R. D. NAYBOUR, *ibid.* **204** (1966) 1200.
24. M. J. HARDING and R. W. K. HONEYCOMBE, *ibid.* **204** (1966) 259.

Received 8 July
and accepted 12 August 1985